Electronic Supplementary Material (ESI) for Journal of Materials Chemistry A.
This journal is © The Royal Society of Chemistry 2020

Supporting Information

Light-gated Cation-selective Transport in Metal-organic Framework Membranes

Hong-Qing Liang, Yi Guo, Xinsheng Peng*, Banglin Chen*

Experimental Section

Materials: Zinc nitrate ($Zn(NO_3)_2 \cdot 6H_2O$) and 2-aminoethanol were purchased from Acros Chemicals. 2-methylimidazole (Hmim) and 1,2,3,3-Tetramethyl-3H-indolium iodide were obtained from Sigma-Aldrich. Ethanol, methanol and piperidine were purchased from Sinopharm Chemical Reagent Co. Ltd. Sodium salicylaldehyde-5-sulfonate was supplied by Chendu Xinhong Material Science & Technology Ltd. China. The substrates were anodic alumina oxide (AAO) membranes (Whatman) with an average pore size of ca. 200 nm and porosity of 50%. Ultrapure water of 18.2 MΩ produced by a Millipore direct-Q system was used throughout the experiments.

Synthesis of 1′,3′,3′-Trimethylspiro[2H-l-benzopyran-2,2′-indoline]-6-sulfonic acid (Sulfated spiropyran): 1,2,3,3-Tetramethyl-3H-indolium iodide (602.3 mg, 2 mmol), sodium salicylaldehyde-5-sulfonate (448.3 mg, 2 mmol), and piperidine (200 μL, 2 mmol) were dissolved in 20 mL methanol. The solution was refluxed for 4 h. The solvent was removed by evaporation under reduced pressure. The residue was dissolved in chloroform and recrystallized by adding benzene. The precipitate was collected and washed by benzene. Purple solid was obtained after dried under reduced pressure (458 mg, yield 60.4%). ^{1}H NMR (600 MHz, DMSO): δ 8.23 (d, J = 2.80 Hz, 1 H), 8.00 (dd, J = 8.99, 2.89 Hz, 1 H), 7.41 (dd, J = 8.08, 1.65 Hz, 1 H), 7.33 (d, J = 1.48 Hz, 1 H), 7.24 (d, J = 10.55 Hz, 1 H), 6.95 (d, J = 8.90 Hz, 1 H), 6.54 (d, J = 8.08 Hz, 1 H), 6.02 (d, J = 10.72 Hz, 1 H), 2.68 (s, 3 H), 1.23 (s, 3 H), 1.13 (s, 3 H).

Fabrication of SSP@ZIF-8 Membranes on AAO: Typically, zinc hydroxide nanostrands (ZHNs) were synthesized by quickly mixing equal volume 4×10^{-3} M zinc nitrate water–ethanol

(water/ethanol volume ratio 3:2) solution with 1.6×10^{-3} M 2-aminoethanol water–ethanol (water/ethanol volume ratio 3:2) solution at room temperature and aging for at least 30 min. 5 mL ZHNs solution was stirring mixed with certain SSP aqueous solution. Then SSP/ZHNs composite thin film was obtained by filtering the mixture onto an AAO membrane. Subsequently, SSP@ZIF-8 membrane was successfully achieved by immersing the SSP/ZHNs thin film into 25×10^{-3} M Hmim water–ethanol (water/ethanol volume ratio 4:1) solution at room temperature for 24 h. Before testing, the membrane was washed with water–ethanol (water/ethanol volume ratio, 4:1) solution three times and dried at room temperature. To investigate the SSP amount effect, 0.31 mL 0.003 wt%, 0.15 mL 0.03 wt%, 0.31 mL 0.03%, and 0.61 mL 0.03 wt% SSP solution were used. The corresponding membranes are denoted as SSP@ZIF-8-1%, SSP@ZIF-8-5%, SSP@ZIF-8-10% and SSP@ZIF-8-20%, respectively.

Characterization: Morphologies were examined by field emission scanning electron microscopy (FESEM, Hitachi S4800, Japan) equipped with X-ray energy dispersive analysis. Fourier transform infrared spectroscopy (FTIR, TENSOR 27) and X-ray photoelectron spectroscopy (XPS, Thermo Scientific, K-Alpha) were used to characterize the surface composition of the membranes. The phase of the as-prepared membranes was characterized by powder X-ray diffraction (XRD) at 0.02 degree step at room temperature using an X'Pert PRO (PANalytical, Netherlands) instrument with Cu Kα radiation. The N_2 sorption isotherms at 77 K were measured by Micromeritics instrument (3Flex) after activating at 100 °C for 12 h. The ^{1}H-NMR spectra was recorded on a 600 MHz NMR spectrometer (Agilent, DD2-600). UV−vis spectrometry (UV2450, Shimadzu, Japan) was used to characterize the photo-isomerization of SSP solutions and SSP@ZIF-8 membranes.

Simulation: All the calculations were performed by using Orca 4.0. The geometries of MC, SP forms and their complexes with the metal ions were optimized by density functional theory (DFT), BLYP functional with D3BJ dispersion and geometrical counterpoise correction (gCP), def2-SVP basis set, and def2/J auxiliary basis set.[1-5] The corresponding single energy calculations were performed by DFT, BLYP functional with D3BJ dispersion, def2-QZVPP basis set and def2/J

auxiliary basis set. The single energies of cations were calculated using CCSD(T)/def2-QZVPP method. The binding energies (E_b) of cations to the two isomerization forms of SSP are calculated as $E_b = E_{isomer\text{-}cation} - E_{isomer} - E_{cation}$, where E_{isomer}, E_{cation} and $E_{isomer\text{-}cation}$ are the energies of the two isomerization forms of SSP (MC or SP), cation, and their complex, respectively.

Ion Conductivity Evaluation: Two Au electrodes were evaporated onto the surface of the membrane on AAO by ZHD-300S film preparation system (BEIJING TECHNOL CO. LTD) with current of 75 A. The total length of the gap between the Au electrodes is 3 mm and the gap width is 300 μm. Two wires were then connected to the electrodes using conductive silver adhesives. The membranes were then sealed by PDMS and used as membrane-based devices for ionic conductive measurement. Typically, the membranes were cut into rectangular pieces and immersed into a blend of PDMS prepolymer and curing agent. After curing, a reservoir was carved out in the PDMS device away from the Au electrodes to expose the membrane to the ions solutions (Figure S8). After immersion in the ionic solution for 12 h, the conductivity of the membrane-based devices was conducted using CHI 660D electrochemical workstation at the mode of alternative current impedance in the frequency range 1 MHz–100 Hz at AC amplitude of 0.5 V. LiCl, NaCl, KCl and $MgCl_2$ aqueous solution with concentrations of 0.5 M were used, of which the pH values are 6.6, 6.8, 6.9, 6.1, respectively. To investigate the effect of light exposure on the conductivity, a 150 W Xe lamp (LOT Oriel) equipped with a 400 nm filter was used as the light source, and the intensity (100 mW cm^{-2}) was calibrated with a standardized silicon solar cell (PV Measurements, USA). The ionic conductivity was calculated based on the equation as follows:

$$\sigma = L/RA \quad (1)$$

where σ is the conductivity, L is the channel length, R is the resistance calculated from electrochemical impedance spectra, and A is the cross-section area of the flow transportation surface.

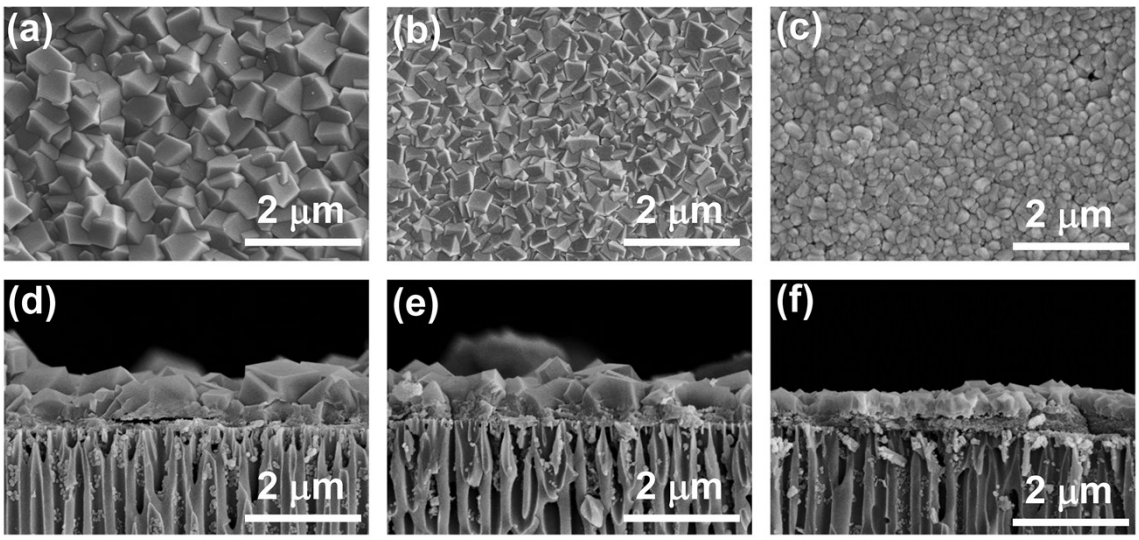

Figure S1. The surface and cross-sectional SEM images of (a,d) SSP@ZIF-8-1%, (b,e) SSP@ZIF-8-5% and (c,f) SSP@ZIF-8-20%.

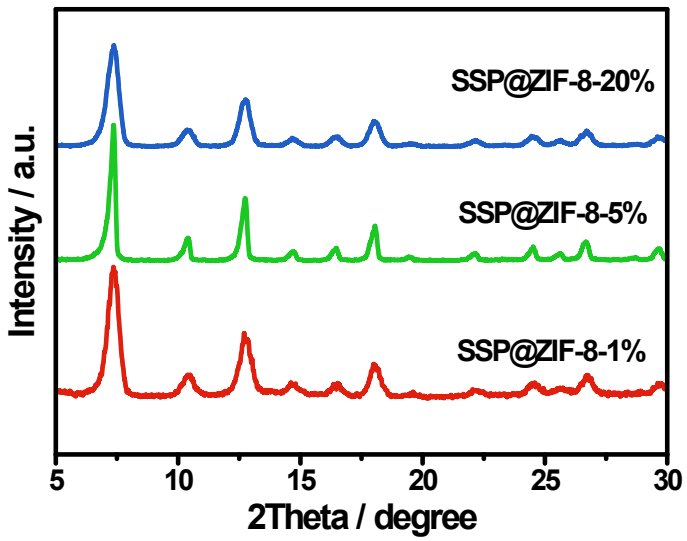

Figure S2. XRD patterns of SSP@ZIF-8-1%, SSP@ZIF-8-5%, SSP@ZIF-8-20% membranes.

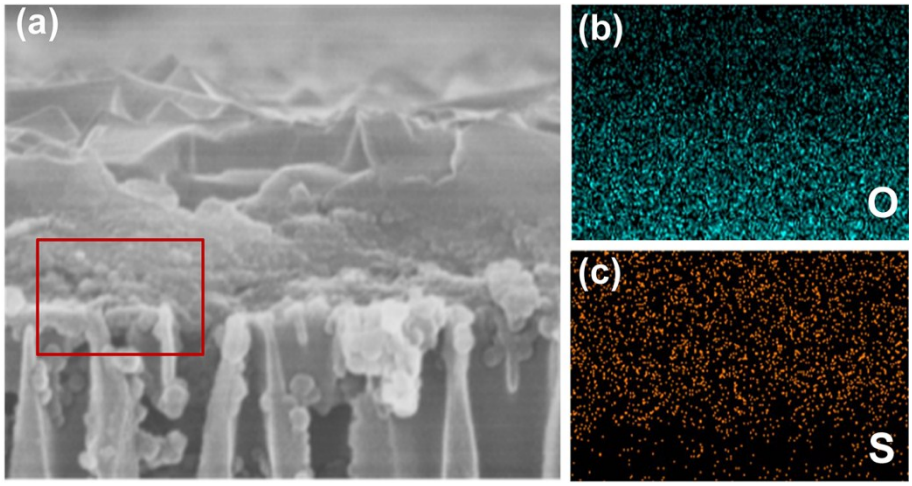

Figure S3. (a) Cross-sectional SEM image of SSP@ZIF-8-10% membranes. O element (b) and S element (c) EDS mapping of (a).

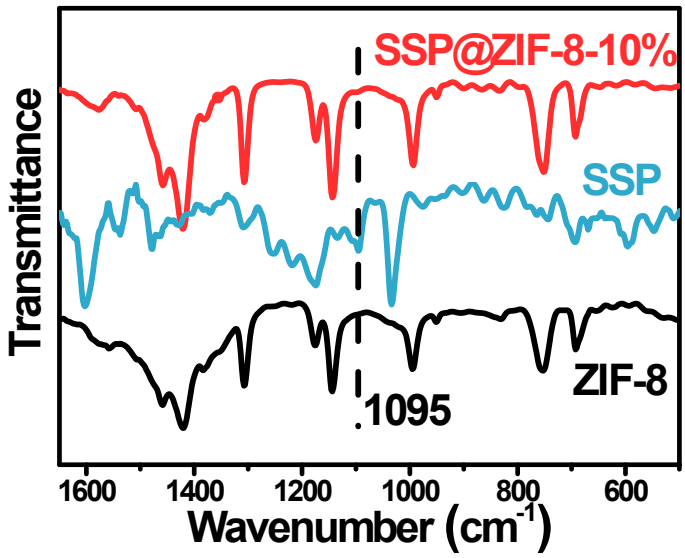

Figure S4. FTIR spectra of ZIF-8, SSP (SP form) and SSP@ZIF-8-10% membranes.

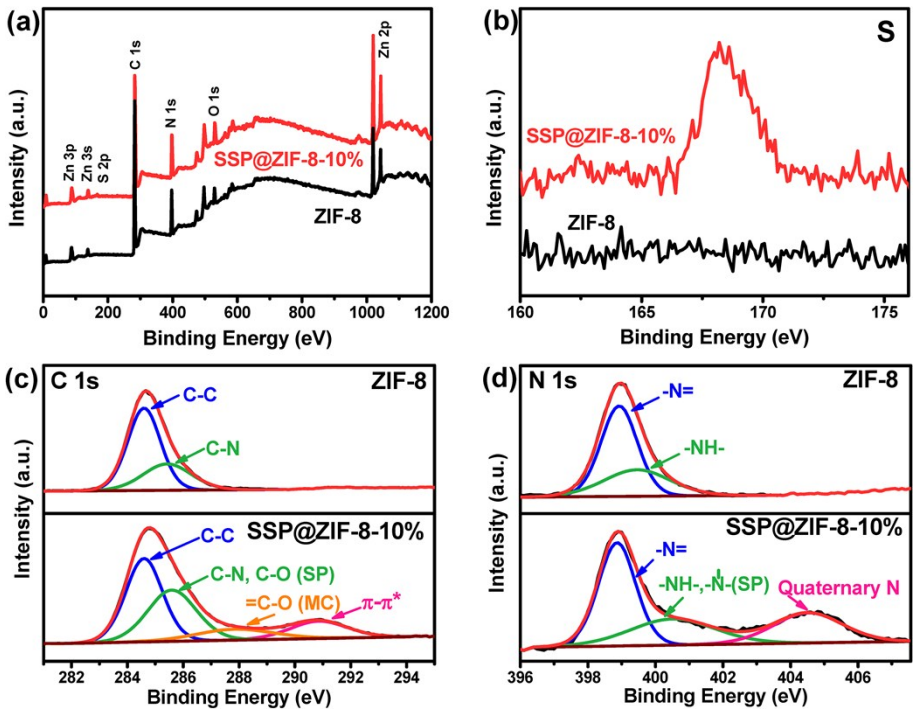

Figure S5. XPS spectra of ZIF-8 and SSP@ZIF-8-10%: wide scan (a) and high-resolution spectra of S 2p (b), C 1s (c), and N 1s (d). In (c), the fitted peaks correspond to C-C (284.6 eV), C-N and C-O in SP form (285.6 eV), =C-O (MC form, 287.8 eV), and π-π* satellite shake-up (290.9 eV). In (d), the fitted peaks correspond to pyridinic N (398.8 eV), pyrrolic N (400.5 eV) and quaternary N (404.5 eV).[6-8]

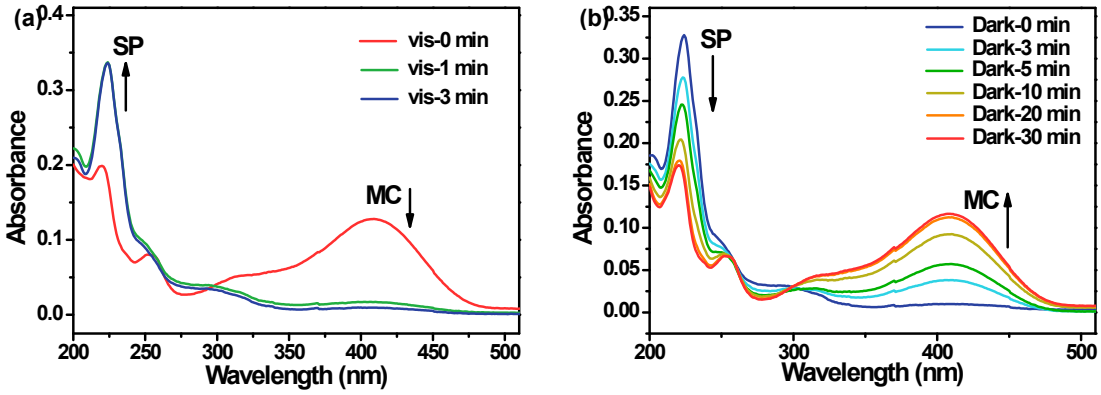

Figure S6. UV-vis absorption spectra of sulfonated spiropyran in an aqueous buffered solution (pH 5) at 298 K. (a) Time evolution on visible light irradiation for 0-3 min. (b) Time evolution in the dark for 0-30 min.

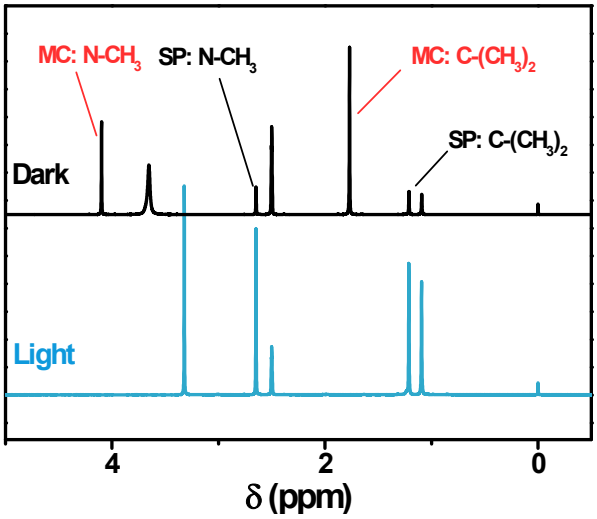

Figure S7. NMR spectra of sulfonated spiropyran in *d*-DMSO at 293 K. Upper (Black line): the thermal equilibrium state (MC) after storing in the dark for 24 h. Bottom (blue line): the SP form after irradiating sufficient visible light. The signals at δ 1.13, 1.23 correspond to the hydrogens in C-$(CH_3)_2$ of SP form, whereas the signals at 1.77 correspond to the hydrogens in C-$(CH_3)_2$ of MC form. The signals at δ 2.68 and 4.10 are assigned to the hydrogen in N-CH_3 of SP form and MC form, respectively. Accordingly, only SP form exists after sufficient visible light irradiation, whereas the MC and SP forms coexist after storing in the dark with the ratio of 71.4: 28.6.[9]

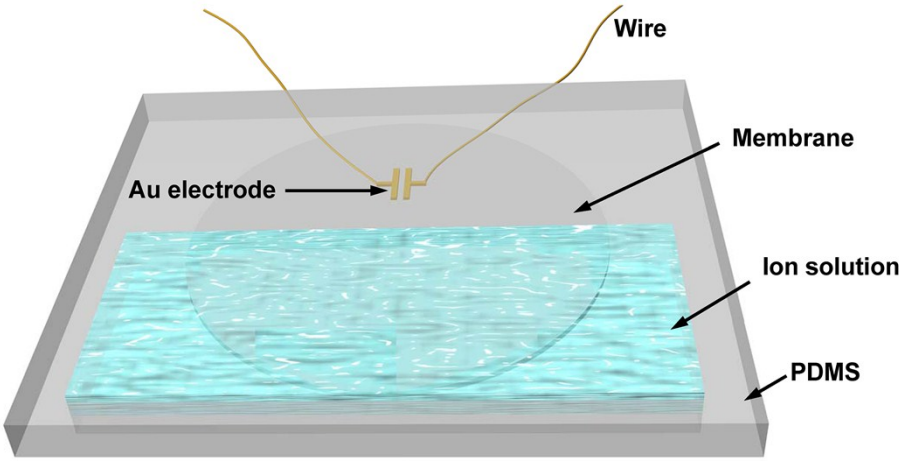

Figure S8. Schematic illustration of the membrane-based device for ionic conductivity test.

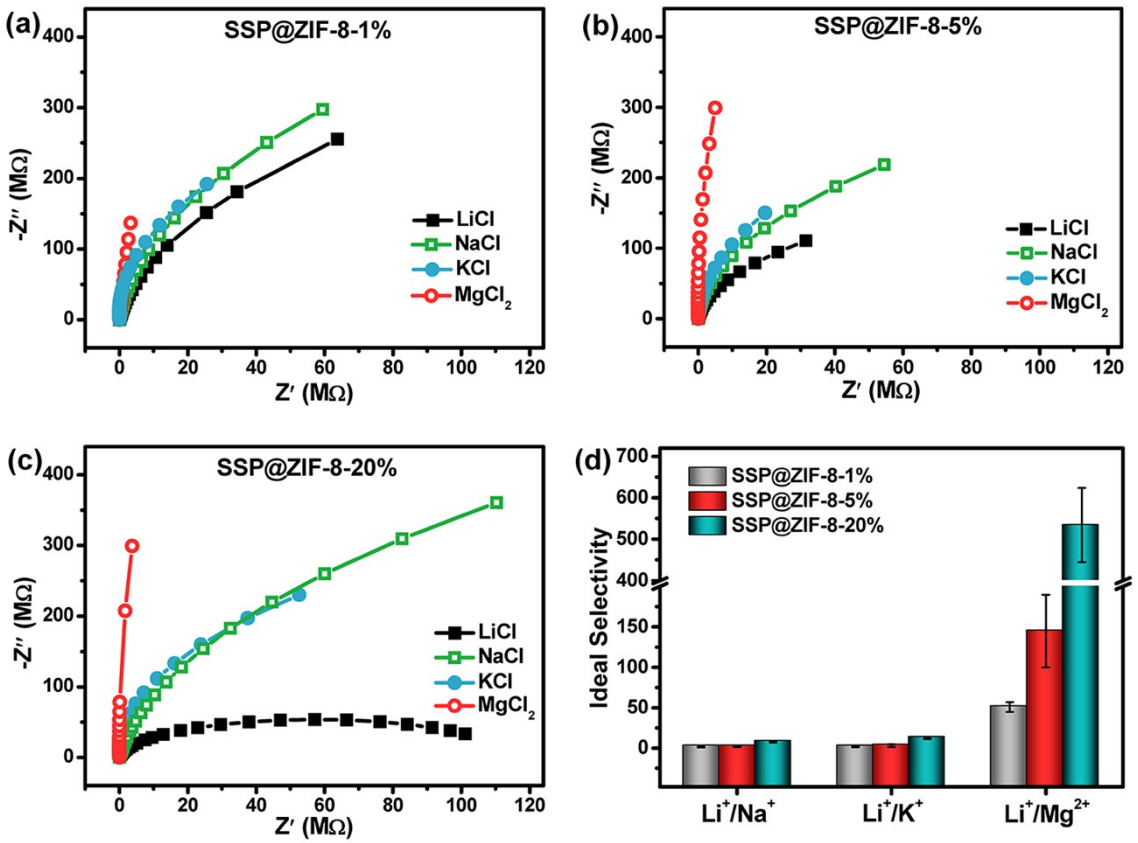

Figure S9. Ion conduction and separation performances of SSP@ZIF-8-1%, SSP@ZIF-8-5%, and SSP@ZIF-8-20% membranes in the dark. (a-c) Nyquist plots of membranes measured with different metal ions: SSP@ZIF-8-1% (a), SSP@ZIF-8-5% (b), SSP@ZIF-8-20%, (c) SSP@ZIF-8-20%. (d) Ideal selectivity for Li^+/Na^+, Li^+/K^+, Li^+/Mg^{2+}.

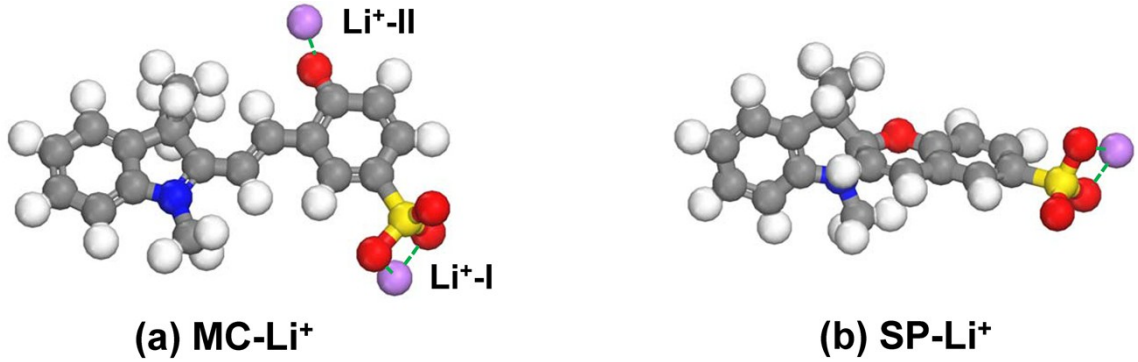

Figure S10. Simulated Li^+ favorable binding sites in MC form (a) and SP form (b).

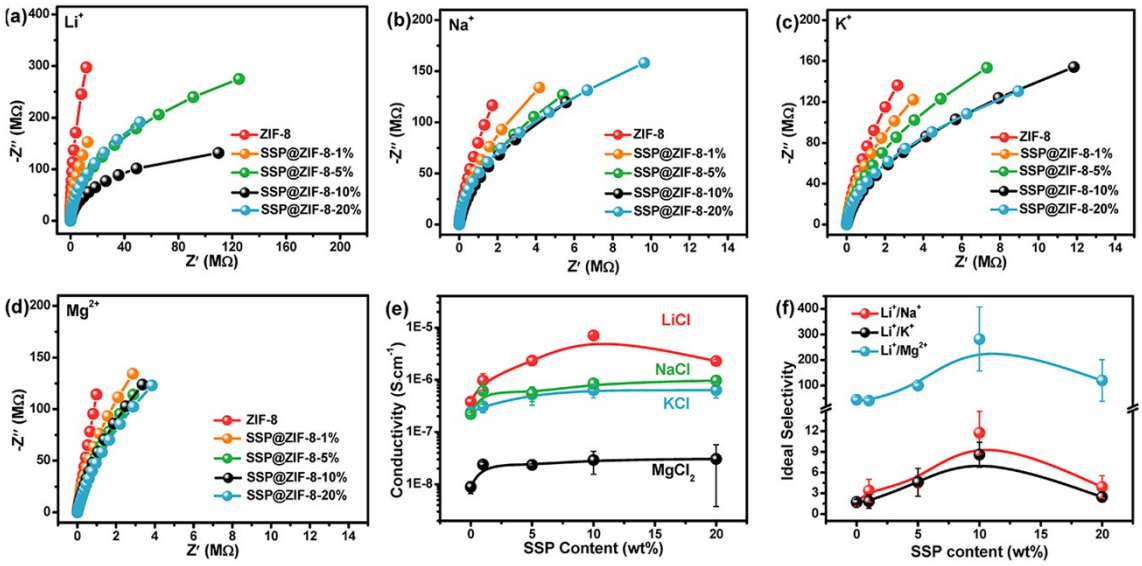

Figure S11. Ion conduction and separation performances of ZIF-8 and SSP@ZIF-8 membranes upon irradiation with visible light. (a-d) Nyquist plots of ZIF-8 and SSP@ZIF-8 membranes measured in metal ion aqueous solution. (a) 0.5 M LiCl, (b) 0.5 M NaCl, (c) 0.5 M KCl, and (d) 0.5 M $MgCl_2$. (e) Ion conductivities through ZIF-8 membrane and SSP@ZIF-8 membranes in different metal ion aqueous solution, calculated from the corresponding Nyquist plots. (f) Ideal selectivity of ZIF-8 membrane and SSP@ZIF-8 membranes.

Table S1 Surface areas and pore volumes of SSP@ZIF-8 membranes with different SSP contents from BET results.

Materials	Surface area ($m^2 \cdot g^{-1}$)	Pore volume ($cm^3 \cdot g^{-1}$)	Specific SSP content (wt%)[a]
ZIF-8	1728.8	0.72	0
SSP@ZIF-8-1%	1705.9	0.71	0.5%
SSP@ZIF-8-5%	1492.0	0.63	6.7%
SSP@ZIF-8-10%	1485.7	0.61	8.1%
SSP@ZIF-8-20%	1436.6	0.60	8.3%

[a] The data was calculated from the variation of pore volumes from pristine ZIF-8.

Table S2 Comparison of the ion selectivity of the SSP@ZIF-8-10% membranes with other synthetic membranes.

Membranes	Channel Length (μm)	Selectivity			Reference
		Li^+/Na^+	Li^+/K^+	Li^+/Mg^{2+}	
SSP@ZIF-8-10%	**300 μm**	**77**	**112**	**4913**	**This work**
sulfonated poly (ether sulfone) cation exchange membranes	~100 μm	0.8	N/A	N/A	[10]
Polyethersulfone/sulfonated poly(phenyl ether ketone)/liquid-liquid membrane	~100 μm	N/A	N/A	>1000	[11]
Polyamide Nanofitration membrane/N90	~100 μm	~1	N/A	~300	[12]
PET/P(AA-co-DEGMEM) membrane	N/A	1.08	1.04	N/A	[13]
Multichannel PET	12 μm	10.5	16.0	634.0	[14]
MXene	1.5 μm	0.9	1.5	8.8	[15]
ZIF-8 membranes	~446 nm	1.4	2.2	N/A	[16]
UIO-66/PET single channel	12 μm	1.2	1.6	N/A	[16]
PSS@HKUST-1	5 mm	35	67	1815	[17]
UiO-66-$(COOH)_2$ in PET nanochannel	N/A	0.49	0.31	1590.1	[18]

References:

1. H. Kruse and S. Grimme, *J. Chem. Phys.*, 2012, **136**, 154101.
2. S. Grimme, S. Ehrlich and L. Goerigk, *J. Comput. Chem.*, 2011, **32**, 1456-1465.
3. S. Grimme, J. Antony, S. Ehrlich and H. Krieg, *J. Chem. Phys.*, 2010, **132**, 154104.
4. F. Weigend and R. Ahlrichs, *Phys. Chem. Chem. Phys.*, 2005, **7**, 3297-3305.
5. F. Weigend, *Phys. Chem. Chem. Phys.*, 2006, **8**, 1057-1065.
6. J. Allouche, A. Le Beulze, J.-C. Dupin, J.-B. Ledeuil, S. Blanc and D. Gonbeau, *J. Mater. Chem.*, 2010, **20**, 9370-9378.
7. V.-D. Dao, N. T. Q. Hoa, L. L. Larina, J.-K. Lee and H.-S. Choi, *Nanoscale*, 2013, **5**, 12237-12244.
8. M. Jiang, X. Cao, D. Zhu, Y. Duan and J. Zhang, *Electrochim. Acta*, 2016, **196**, 699-707.
9. A. Sugahara, N. Tanaka, A. Okazawa, N. Matsushita and N. Kojima, *Chem. Lett.*, 2014, **43**, 281-283.
10. H. J. Cassady, E. C. Cimino, M. Kumar and M. A. Hickner, *J. Membr. Sci.*, 2016, **508**, 146-152.
11. J. Song, X.-M. Li, Y. Zhang, Y. Yin, B. Zhao, C. Li, D. Kong and T. He, *J. Membr. Sci.*, 2014, **471**, 372-380.
12. A. Somrani, A. H. Hamzaoui and M. Pontie, *Desalination*, 2013, **317**, 184-192.
13. A. R. Garifzyanov, N. V. Davletshina, A. R. Garipova and R. A. Cherkasov, *Russ. J. Gen. Chem.*, 2014, **84**, 285-288.
14. Q. Wen, D. Yan, F. Liu, M. Wang, Y. Ling, P. Wang, P. Kluth, D. Schauries, C. Trautmann, P. Apel, W. Guo, G. Xiao, J. Liu, J. Xue and Y. Wang, *Adv. Funct. Mater.*, 2016, **26**, 5796-5803.
15. C. E. Ren, K. B. Hatzell, M. Alhabeb, Z. Ling, K. A. Mahmoud and Y. Gogotsi, *J. Phys. Chem. Lett.*, 2015, **6**, 4026-4031.
16. H. Zhang, J. Hou, Y. Hu, P. Wang, R. Ou, L. Jiang, J. Z. Liu, B. D. Freeman, A. J. Hill and H. Wang, *Sci. Adv.*, 2018, **4**, eaaq0066.
17. Y. Guo, Y. Ying, Y. Mao, X. Peng and B. Chen, *Angew. Chem. Int. Ed.*, 2016, **55**, 15120-15124.
18. J. Lu, H. Zhang, J. Hou, X. Li, X. Hu, Y. Hu, C. D. Easton, Q. Li, C. Sun, A. W. Thornton, M. R. Hill, X. Zhang, G. Jiang, J. Z. Liu, A. J. Hill, B. D. Freeman, L. Jiang and H. Wang, *Nature Materials*, 2020, DOI: 10.1038/s41563-020-0634-7.